

# LAPW frozen-phonon calculation, shell model lattice dynamics and specific-heat measurement of SnO

S. Koval<sup>a \*</sup>, R. Burriel<sup>b</sup>, M.G. Stachiotti<sup>a</sup>, M. Castro<sup>b</sup> R.L. Migoni<sup>a</sup>, M.S. Moreno<sup>d †</sup>, A. Varela<sup>d</sup> and C.O. Rodriguez<sup>e</sup>

<sup>a</sup> *Instituto de Física Rosario, Universidad Nacional de Rosario,  
27 de Febrero 210 Bis, 2000 Rosario, Argentina.*

<sup>b</sup> *Instituto de Ciencia de Materiales de Aragón, CSIC, Universidad de Zaragoza,  
Plaza de San Francisco, 50009 Zaragoza, Spain.*

<sup>c</sup> *Departamento de Física, TENAES, Universidad Nacional de La Plata,  
C.C. 67, 1900 La Plata, Argentina.*

<sup>d</sup> *Dpto. de Química Inorgánica, Facultad de Ciencias Químicas, Universidad Complutense,  
28040 Madrid, Spain.*

<sup>e</sup> *IFLYSIB, Grupo de Física del Sólido, C.C.565, 1900 La Plata, Argentina.*

## Abstract

An ab-initio Linear Augmented Plane-Wave (LAPW) calculation of the zone-centered phonon frequencies of SnO has been performed.  $E_g$  symmetry has been ascribed to the mode observed at  $113\text{ cm}^{-1}$  in Raman measurements, discarding a previous  $B_{1g}$  assignment. The other phonon modes measured by Raman spectroscopy are also well reproduced. A new shell-model has also been developed, that gives good agreement of the zone-centered frequencies compared to the measured data and the LAPW results. Specific heat measurements have been performed between 5 K and 110 K. Computation of the specific heat and

---

\*Present address: International Centre for Theoretical Physics, Strada Costiera 11, 34014, Trieste, Italy.

†Present address: Goldaracena 740, 2820 Gualeguaychu (Entre Rios), Argentina

the Mössbauer recoilless fraction with the improved shell-model shows a good agreement with the experimental data as a function of temperature.

PACS numbers: 63.20.Dj, 76.80.+y

SnO has not been subject of extensive investigations due to its thermal decomposition at relatively low temperatures, precluding applications. Presently it is object of a renewed interest, due to its ability to be an excellent anode material [1] and, so far, there is no confident description of its vibrational structure. Very recently, three contributions were concerned with an appropriate description of its electronic properties [2–4]. However, a proper description of its phonons and lattice dynamics is absent.

A shell model for the lattice dynamics of SnO has been developed recently with the aim to analyse the Mössbauer recoilless fraction of Sn [5]. The resulting zone center phonon frequencies have been compared with ab-initio full potential linear-muffin-tin-orbital (LMTO) calculations [4] and Raman and infrared reflectivity measurements [6]. The agreement was in general good for the Mössbauer data as well as for the phonon frequencies. However, the latter showed some discrepancies. On one hand, the analysis of the experimental data assigned the  $B_{1g}$  symmetry to a Raman peak at  $113\text{ cm}^{-1}$ , while both the LMTO and shell model calculations gave a frequency of  $\approx 370\text{ cm}^{-1}$  for the  $B_{1g}$  mode. Since this mode involves only oxygen displacements, it is hard to believe that it has such a low frequency as experimentally assigned, because there are other Sn-modes with higher frequencies. This inconsistency in the assignment of the  $113\text{ cm}^{-1}$  Raman peak remained unnoticed even in the most recent works [7]. On the other hand, the lowest frequency mode is of  $E_g$  symmetry, involving mainly Sn displacements, and has a frequency of 160 or  $143\text{ cm}^{-1}$  according to the shell model [5] or the LMTO [4] calculation, respectively. An additional discrepancy appears for the  $A_{2u}$  mode, which has a frequency of  $255\text{ cm}^{-1}$  for the shell model, while the LMTO calculation leads to a value of  $396\text{ cm}^{-1}$ , and no experimental data is available for this mode.

In order to elucidate these questions we undertake in this work a full potential LAPW calculation of the zone-center modes, which is more confident than the LMTO method for the calculation of phonon energies, particularly in the quite open structure of SnO. We then refine the shell model parameters by fitting them to the LAPW results and the spectroscopic experimental data. In addition, we present measurements of the specific heat, which will allow to check the consistency of the determined shell-model parameters. We remark that the development of a reliable model of SnO should be interesting for the study of the tweed

microstructure associated with this intrinsically non-stoichiometric compound [8].

The ab-initio calculations were performed within the Local Density Approximation (LDA) to density functional theory, using the full-potential LAPW method. In this method no shape approximation on either the potential or the electronic charge density is made. We use the WIEN95 implementation of the method [9] which allows the inclusion of local orbitals (LO) in the basis, making possible a consistent treatment of semicore and valence states in one energy window hence insuring proper orthogonality [10]. The Ceperley-Alder parametrization for the exchange-correlation potential is used [11].

The atomic sphere radii ( $R_i$ ) 2.15 and 1.60 a.u. were used for Sn and O, respectively. For the parameter  $RK_{max}$ , which controls the size of the basis sets in these calculations, we take the value of 8. This gives well converged basis sets consisting of approximately 990 LAPW functions plus local orbitals. We introduce LO to include the following orbitals in the basis set: Sn  $4p$  and  $4d$ , and O  $2s$ .

Integrations in reciprocal space were performed using the tetrahedron-method. We used  $7 \times 7 \times 5$  meshes which represent 30  $k$ -points in the irreducible Brillouin zone.

We determined the phonon frequencies and eigenvectors of particular symmetry using the frozen phonon approach, by calculating atomic forces for several small displacements ( $u \approx 0.3\%$  of the lattice constant) consistent with the symmetry and small enough to be in the linear regime. From the forces as a function of displacements the dynamical matrix was constructed and diagonalized.

We observe in Table I that in general the LAPW-frequencies are somewhat smaller than the LMTO values. The LAPW result for the  $E_u$  mode is in better agreement with the experiment than the LMTO result. The lowest mode is confirmed to be of  $E_g$  symmetry as in the LMTO calculation [4], although it lies considerably lower in frequency. The present LAPW calculation leads to a frequency for this mode in exact agreement with the position of the peak observed in the Raman experiment [6]. However the experimental analysis leads to an identification of this peak as arising from the  $B_{1g}$  mode. We believe that this assignment is wrong on the basis of several grounds. First, both ab-initio calculations already mentioned predict the  $E_g$  symmetry for the lowest frequency mode. Second, the  $B_{1g}$  mode involves only antiparallel  $z$ -displacements

of O ions, while the  $A_{1g}$  mode is the analogous for the Sn ions. Both modes are determined by Sn-O interactions, while the Sn-Sn and O-O forces play an additional role in the  $A_{1g}$  and the  $B_{1g}$  modes, respectively. Therefore, as long as the Sn-O interaction is dominant (as it comes out from the LAPW calculations and shell model results which will be described latter), the higher frequency mode will be the one corresponding to movements of lighter atoms, i.e. the  $B_{1g}$  mode. Third, for the isostructural compound  $PbO$ , the measured frequency of the  $B_{1g}$  mode [12] is close to the calculated value for tin monoxide.

The frequency of the  $A_{2u}$  mode could not be confidently determined. As a consequence of the general underestimation of the electronic band gap within the LDA, we obtain a very small band gap for SnO. When the atoms are displaced according to the  $A_{2u}$  eigenvector pattern, part of the conduction band crosses below the top of the valence band and thus becomes populated. This affects the displacement dependence of the energy, which leads to an unreliable frequency value of this phonon. The same problem arises from the LMTO calculation, which is based also on the LDA, so that the previously published value is also unreliable. [4]

Now we improve the shell model of Ref. [5]. It contains short range shell-shell interactions of the Buckingham form for the nearest neighbor pairs O-O and Sn-O and up to second neighbors for the Sn-Sn pair, as well as long range Coulomb interactions among all ions. Starting from the parameter values given in Ref. [5] we further fitted them to the new LAPW results, in addition to the experimental phonon data. The most significant differences, which appeared for the  $E_g$  modes, could be corrected by modifying the O-O interaction potential and the O polarizability. We also adjusted slightly the Sn-O interaction to improve the fitting. With the parameter set shown in Table II we obtain the zone-center phonon frequencies shown in Table I. A good agreement with the LAPW results is achieved. Also the experimental data are well reproduced, except for the  $113\text{ cm}^{-1}$  experimental phonon data, as previously discussed. Considering the experimental values for the  $E_u$  and  $A_{1g}$  modes and the LAPW values for the remaining zone center modes we obtain a RMS frequency difference of  $7\text{ cm}^{-1}$  with our shell model result. The shell model phonons are stable throughout the Brillouin zone.

In order to validate the present shell model with experimental data we use it to compute both the Mössbauer recoilless fraction and the phonon density of states (PDOS) which allows a

direct calculation of the specific heat. The Mössbauer recoilless fraction  $f(T)$  calculated with the present model shows no significant difference with the previous calculation [5].

The specific heat of SnO has been measured in a commercial adiabatic calorimeter from Termis Ltd. [13] between 5 K and 110 K. An amount of 2 g of a finely grounded sample was sealed in the 1 cc sample container with 50 mbar of He gas to improve the heat exchange and temperature equilibrium. Below 5 K the helium gas was absorbed on the sample surface preventing to reach thermal equilibrium within measurable times. Carbon-glass and Rh-Fe thermometers were used on the sample holder and on the adiabatic shield that surrounds it. The temperature of the shield is controlled to follow the sample temperature providing adiabatic conditions. The sample specific heat was obtained after subtracting the empty sample holder contribution measured on a previous experiment. The experimental values, shown in Fig. 1a, present a characteristic maximum at 10 K in the  $C_p/T^3$  vs.  $T$  representation. The effective Debye temperatures, derived from the calorimetric data, have been represented in Fig. 1b.

From the calculated PDOS we derived the molar heat capacity using the following expression:

$$C_v(T) = 3nR \int_0^{\omega_{max}} g(\omega) E\left(\frac{\hbar\omega}{k_B T}\right) d\omega \quad (1)$$

where  $n$  is the number of atoms by formula unit,  $R$  is the molar gas constant,  $g(\omega)$  is the normalized PDOS determined by the shell model, and  $E(x)$  is the Einstein function:

$$E(x) = \left(\frac{x/2}{\sinh(x/2)}\right)^2 \quad (2)$$

The low-frequency limit of  $g(\omega)$  has been smoothed by fitting a quadratic law to the histogram, in order to avoid the influence of noise in the evaluation of the heat capacity. To take into account an estimated presence of 10 % Sn vacancies in the employed samples, we use a value  $n = 1.9$  for the evaluation of  $C_v$  according to Eq. (1) as well as for the conversion of the experimental data to molar units. Note that  $C_v \approx C_p$  for a solid, thus we shall compare directly the calculated  $C_v$  with the measured  $C_p$ . The calculated specific heat, shown in Fig. 1a, has the maximum shifted to a higher temperature, 16 K, with a height slightly lower than for the experimental data. A similar behaviour can be seen on the effective Debye temperatures, represented in Fig 1b, with the minimum slightly shifted with respect to the experimental one.

The calculations have a remarkable coincidence with the experimental measurements above 15 K. The whole result is quite good considering that the model corresponds to a perfect solid. Cation vacancies and the elastic relaxation existing in the real solid [8] have not been taken into account in the model. Also the uncertainty in the acoustic and low-frequency modes, which give the most important contribution to the specific heat at low temperature, can account for the difference between calculated and experimental data.

As general features in our calculation, we observe a small Debye region of  $\approx 4$  K (defined as the region where  $\Theta(T) \approx \Theta(T = 0\text{K})$ ) and a large drop ( $\approx 35\%$  of the zero-temperature value) in  $\Theta(T)$  at low temperatures. The origin of these behaviours may be ascribed to a strong hybridization of the acoustic and low frequency optical bands near the center of the Brillouin zone (BZ), which can be observed particularly in the  $(k,k,0)$  symmetry direction (the same result is found in our previous shell model calculation [5]). This hybridization causes on one hand the onset of curvature in the acoustic dispersion curves at quite low frequencies which accounts for the small Debye region mentioned. On the other hand, the mentioned hybridization causes low lying modes towards the end of BZ which are responsible for the large drop in the Debye temperature.

Recently, the partial Sn-PDOS has been obtained from measurements performed in the Advanced Photon Source at the Argonne National Laboratory [14]. The accord with our results is very good in the positions as well as in the height of the peaks. Moreover, this accord, together with the fact that our calculated partial O-PDOS has nearly vanishing spectral weight for frequencies  $\omega < 220 \text{ cm}^{-1}$ , reinforces our conclusion that the oxygen mode of  $B_{1g}$  symmetry was wrongly assigned in Raman experiments [6]. These results will be published elsewhere together with data on other Sn compounds.

Acknowledgements: Partial support from CICYT Project no. MAT97-0987 is acknowledged. Support through fellowships and a grant from the Consejo Nacional de Investigaciones Científicas y Técnicas de la República Argentina is also acknowledged.

## REFERENCES

- [1] Y.Idota, T.Kubota, A.Matsufuji, Y.Maekawa, and T.Miyasaka; *Science* **276**, 1395 (1997).
- [2] I.Lefebvre, M.A.Szymanski, J.Olivier-Fourcade and J.C.Dumas; *Phys. Rev. B* **58**, 1896 (1998).
- [3] M.Meyer, G.Onida, A.Ponchel and L.Reining; *Comput. Mater. Sci.* **10**, 319 (1998).
- [4] E. Peltzer y Blancá, A. Svane, N.E. Christensen, C.O. Rodriguez, O.M. Cappannini and M.S. Moreno; *Phys. Rev. B* **48**, 15712 (1993).
- [5] S. Koval, M.G. Stachiotti, R.L. Migoni, M.S. Moreno, R.C. Mercader and E.L. Peltzer y Blancá; *Phys. Rev. B* **54**, 7151 (1996).
- [6] J. Geurts, S. Rau, W. Richter and F.J. Schmitte; *Thin Solid Films* 121, 217 (1984).
- [7] L.Sangaletti, L.E.Depero, B.Allieri, F.Pioselli, E.Comini, G.Sberveglieri and M.Zocchi; *J.Mater.Res.* **13**, 2457 (1998).
- [8] M.S. Moreno, A. Varela and L.C Otero-Díaz; *Phys. Rev. B* **56**, 5186 (1997).
- [9] P. Blaha, K. Schwarz, P. Dufek and R. Augustyn, WIEN95, Technical University of Vienna 1995. (Improved and updated Unix version of the original copyrighted WIEN-code, which was published by P. Blaha, K. Schwarz, P. Sorantin and S.B. Trickey; *Comput. Phys. Commun.* **59**, 399 1990).
- [10] D. Singh, *Phys. Rev. B* **43**, 6388 (1991).
- [11] D.M. Ceperley and B.J. Alder; *Phys. Rev. Lett.* **45**, 566 (1980).
- [12] D.M. Adams, A.G. Christy, J. Haines, S.M. Clark, *Phys. Rev. B* **46**, 11358 (1992); D.M. Adams and D.C. Stevens, *J. Chem. Soc. Dalton* **1977**, 1097 (1977).
- [13] F. Pavese and V.M. Malyshev, *Adv. Cryogenic Engineering* **40**, 119 (1994).
- [14] M.Y. Hu, W. Sturhahn, T.S. Toellner, E.E. Alp, P.L. Lee, P.M. Hession, S. Koval and R.L. Migoni, unpublished.



# FIGURES

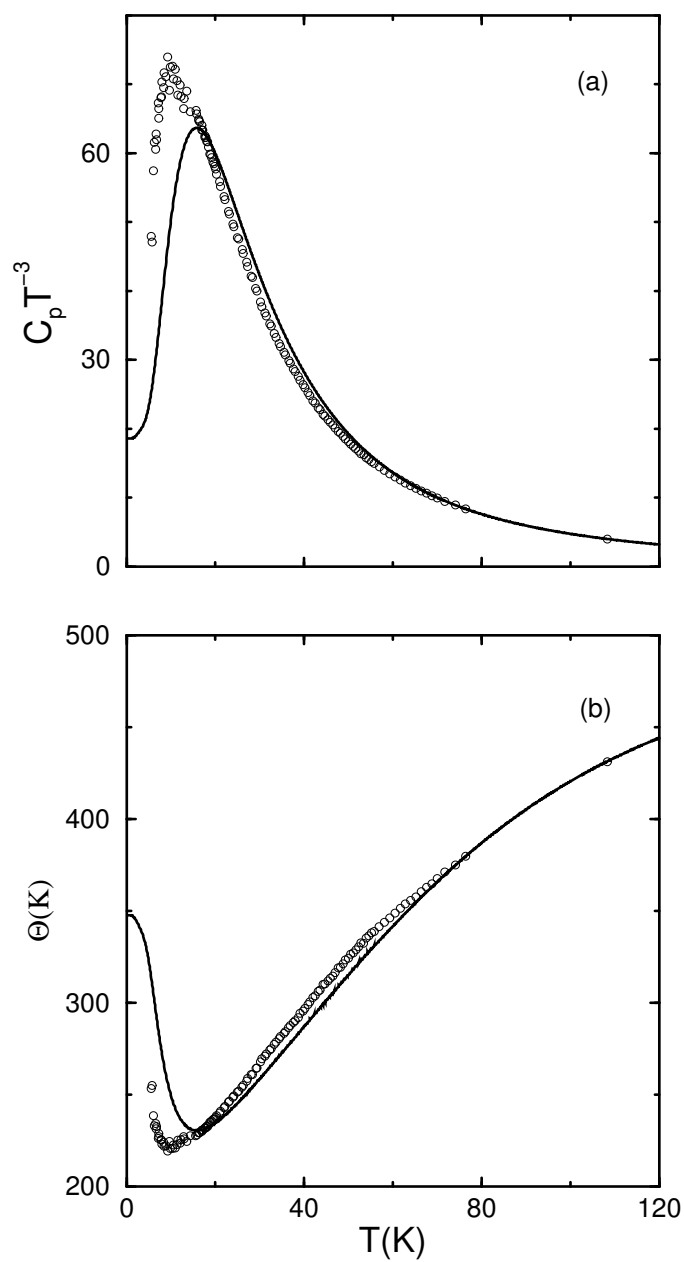


FIG. 1. Specific heat (a) and effective Debye temperature (b) as functions of temperature. Solid line: shell model calculation. Open circles: experimental data. The  $C_p/T^3$  values are given in units of  $10^{-7}5.7R/K^3$

TABLES

TABLE I. Frequencies of the TO zone-center modes of  $SnO$ : for the first-principle LAPW calculation, for the shell model, for the LMTO calculation and for the experiment (Unit:  $cm^{-1}$ ). We also show the relative atomic displacements for each mode, according to the LAPW calculation. A and B symmetries correspond to c-polarized modes, E symmetries to a-polarization.  $+(-)$  means in-phase (out of phase) ionic motions.

Mode	LAPW	Shell Model	LMTO [4]	Experiment [6]	$Sn + Sn$	$O + O$	$Sn - Sn$	$O - O$
$E_g$	460	450	494		0	0	0.023	1
$A_{2u}$		240	396 ?		0	1	0	0
$B_{1g}$	350	357	370	113 ?	0	0	0	1
$E_u$	271	267	296	260	0	1	0	0
$A_{1g}$	212	211	211	211	0	0	1	0
$E_g$	113	122	143		0	0	1	0.17

TABLE II. Parameters of the model:  $a, b, c$ : potential parameters;  $Z, Y$ : ionic and shell charges;  $K$ : on site core-shell force constant;  $A, B$ : longitudinal and transversal force constants between neighboring ions.

Interaction	$a$ (ev)	$b$ ( $\text{\AA}^{-1}$ )	$c$ (eV $\text{\AA}^6$ )	$A(e^2/v_a)$	$B(e^2/v_a)$	Ion	$Z( e )$	$Y( e )$	$K(e^2/v_a)$
Sn-O	528	2.85	0	37.05	-5.9	O	-1.4	-3.5	300.52
Sn-Sn	2309	2.50	0	10.0	-1.1	Sn	1.4	0	$\infty$
O-O	76031	3.925	2000	-0.89	7.27				